

## Simulations of SPERT-IV D12/15 transient experiments using the system code THERMO-T



Marat Margulis, Erez Gilad\*

The Unit of Nuclear Engineering, Ben-Gurion University of the Negev, Beer-Sheva, 84105, Israel

### ARTICLE INFO

#### Keywords:

THERMO-T  
System code  
Transient analysis  
RIA  
SPERT-IV  
Serpent

### ABSTRACT

Best-estimate codes, which couple neutronic and thermal-hydraulic solvers, are mainly used for safety analyses of nuclear power plants. During the past decade, the application of these codes to research reactors gained considerable interest and many improvements were presented to them. The increasing interest in the application of best-estimate codes to safety analyses of research reactor is largely driven by advancements in this field concerning power reactors and the diffusion of knowledge and capabilities to smaller, more diverse systems. The current study is a continuous effort in this framework and presents the coupled neutronic and thermal-hydraulic code development for the analysis of protected and unprotected transient behavior of research reactors. The coupling between neutronic and thermal-hydraulic processes is realized by considering the mutual feedbacks between them; the fuel and coolant properties (temperatures and density) variation affect the core's reactivity and hence the neutronic fission chain reaction, which in turn affects the fuel and coolant properties via a heat generation model for the reactor's power. More specifically, this study deals with the extension of the thermal-hydraulic model to the two-phase flow regime of the THERMO-T code. The extended THERMO-T model is validated against experimental results from the SPERT-IV, which was driven mainly by the coolant density reactivity feedback. This allows a more accurate evaluation of the adequacy of available and relevant two-phase flow models and correlations, which are selected from the domain of large power reactors. This is done in order to encourage and ensure standardization of modeling procedure of all types of reactors as part of the international community's continuous efforts towards this goal.

### 1. Introduction

Research Reactors (RRs) are unique systems that support a variety of nuclear research needs, including basic nuclear physics and neutron physics, neutron diffraction, material properties, radiation studies, health applications, and more. One of the major roles of RRs is to support research needs of commercial nuclear power reactors. The characteristics of RRs are usually more flexible than those of commercial Nuclear Power Plants (NPPs) and they operate at low thermal power levels (usually not exceeding 100 MW<sub>th</sub>) and small core sizes, which lead to high power densities, low temperatures of the fuel and clad, and low system pressure (close to atmospheric). Furthermore, the fuel composition and geometric design can be highly heterogeneous. These unique characteristics lead to a variety of different neutronic and thermal-hydraulic designs (D'Auria and Bousbia-Salah, 2006; Hamidouche et al., 2008; Adorni et al., 2006; Adorni et al., 2007), which dictate a wide range of different and unique safety requirements in order to ensure their safe operation. The diversity of different designs

make the standardization of operation, regulation and licensing almost impractical (Hamidouche et al., 2008; Costa et al., 2011).

A modeling challenge in calculating power excursion transients in RR is to demonstrate that the numerical models are conservative with respect to the safety limits, i.e., provide a sort of “safe side” approach that would ensure overestimation of damage-indicating parameters (i.e., power, cladding temperature). Employing a conservative approach (approximations and correlations) is common practice in NPPs analysis (due to lack of experimental data, among other reasons), which ensure that the design and operation safety margins are not exceeded. In recent years, the international community acknowledged the importance of implementing the established knowledge and methodologies used for NPPs safety analyses to safety analyses of RRs (Hamidouche et al., 2008; Hamidouche et al., 2004; IAEA, 2007; IAEA, 2008).

In order to test the capabilities of different codes and models in analyzing RRs operation and transients, several benchmark problems were proposed by the International Atomic Energy Agency (IAEA). One of the first benchmarks proposed is the 10 MW<sub>th</sub> Material Test Reactor

\* Corresponding author.

E-mail address: [gilade@bgu.ac.il](mailto:gilade@bgu.ac.il) (E. Gilad).

<https://doi.org/10.1016/j.pnucene.2018.07.005>

Received 14 February 2018; Received in revised form 13 June 2018; Accepted 16 July 2018

Available online 20 July 2018

0149-1970/ © 2018 Elsevier Ltd. All rights reserved.

### Acronyms

DNB	Departure from Nucleate Boiling
HEU	Highly Enriched Uranium
IAEA	International Atomic Energy Agency
LOFA	Loss-of-Flow Accident
MC	Monte Carlo

MTR	Material Test Reactor
NEA	Nuclear Energy Agency
NPP	Nuclear Power Plant
RIA	Reactivity Insertion Accident
RR	Research Reactor
SIMPLE	Semi-Implicit Method for Pressure Linked Equations
SPERT	Special Power Excursion Reactor Test

(MTR) (IAEA, 1980; IAEA, 1992), which included information for code verification against burnup calculations, static power and flux distributions and information regarding transient analysis of Reactivity Insertion Accidents (RIA) and Loss-of-Flow Accidents (LOFA) for different fuel compositions (high and low enriched uranium). This benchmark has been introduced in the framework of the Reduced Enrichment for Research and Test Reactors (RERTR) Program. This benchmark is a purely numerical approximation of a hypothesized MTR core, which was utilized for the verification of the system code THERMO-T (Margulis and Gilad, 2016a).

In recent years, the IAEA 10 MW<sub>th</sub> MTR benchmark tends to be considered obsolete to some extent for code validation. This is in view of recent activities of the IAEA and the Nuclear Energy Agency (NEA), which aim at introducing proper benchmark problems that would be based on experimental data deduced from experiments performed in RRs. A series of such benchmarks were made available in the framework of the IAEA CRP 1496 (IAEA, 2013) and published in 2015 as IAEA Technical Reports Series No. 480 (IAEA, 2015). The report contains experimental data gathered from different RRs such as ETRR-2 (Egypt), IEA-R1 (Brazil), Minerve (France), SPERT III and IV (USA), and more. The report includes both RIA and LOFA experimental measured data and is intended to be used as code validation benchmark (Chatzidakis et al., 2013, 2014; Hainoun et al., 2014). This work focuses on the SPERT-IV destructive test series.

The SPERT-IV experiment aimed at studying the unique dynamic behavior of a RR system by the performance and analysis of reactor kinetic experiments. The SPERT-IV D-12/25 core was the final aluminum plate-type core studied as part of the Special Power Excursion Reactor Test (SPERT) project. The experimental details are summarized in section 2. The experiments were designed to push the RR system to its limits, with the final experiment of a complete withdrawal of all the control rods. The characteristics of the experiment provide a good (yet challenging) platform for the evaluation of the two-phase flow models utilized in the different codes. This is a result of the utilization of Highly Enriched Uranium (HEU) fuel, which practically eliminates the Doppler reactivity coefficient and emphasizes reactivity coefficient of the coolant/moderator.

The main goal of this paper is to estimate the performance of the correlation implemented in the THERMO-T system code (Margulis and Gilad, 2015, 2016b). In previous studies, the THERMO-T was compared to state of the art codes such as RELAP5, PARET, RETRAC-PC, and COBRA-EN, in the frame of the IAEA 10 MW<sub>th</sub> MTR benchmark (Margulis and Gilad, 2016b). However, those studies did not include two-phase flow capabilities comparison nor did they include any experimental measured data. Thus, in support of the IAEA activities, the focus in this article is put on the utilization of common practice methodology for the analysis of two-phase flow in commercial power systems (Todreas and Kazimi, 1990a) in the THERMO-T system code for RRs analysis. This is made through the validation of those models against experimental data available from SPERT-IV program.

The current work falls in line with efforts of the nuclear community to utilize experimental data for code validation, lead by the activities of the IAEA and the OECD's Nuclear Energy Agency (NEA). In recent years, as a result of the activities of the two agencies, a substantial experimental data for code validation became available (IAEA, 2015; NEA, 2017), and more data to become available in the near future, e.g.,

the BEAVRS (Horelik et al., 2013), MSRE (Fratoni, 2017) and SNEAK-12 (Margulis et al., 2017) benchmark problems. However, efforts to produce higher quality experimental data for codes and design validation are constantly under investigation. For example, high representative experimental programs that will provide reactor designers and operators with experimental feedback. One such a program is currently under investigation in a collaboration between CEA Cadarache and Ben-Gurion University of the Negev on the studies of neutronic characteristics during severe accidents in Gen-IV reactors (Margulis et al., 2018).

## 2. Methodology

This section summarizes the tools, methods and models that are utilized in this work. It includes a short description of the SPERT-IV core, a short description of the Serpent Monte Carlo (MC) code and an overview of the THERMO-T code extended to two-phase flow and heat transfer models.

### 2.1. SPERT-IV d-12/25

SPERT-IV was a light water cooled and moderated pool-type reactor, with upward forced and natural convection cooling. The core was composed of 25 fuel assemblies, 20 standard, and 5 control fuel assemblies. The different fuel assemblies are placed in a  $5 \times 5$  section of the  $9 \times 9$  support grid, as shown in Figs. 1 and 2. The reactor was loaded with highly enriched uranium (HEU) plate-type fuel cased in an aluminum cladding ( $UAl_x-Al$ ). Each standard fuel assembly contained 12 fuel plates, housed in an aluminum assembly can. The four control assemblies and the single transient rod are made of double-blade control rods of the same style, but with a different operational direction. The control rods were extracted in the upward direction, while the

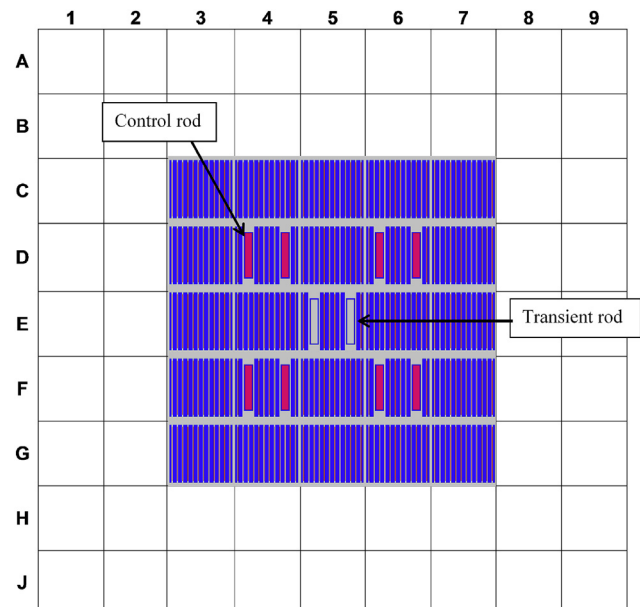


Fig. 1. Schematic representation of the SPERT-IV D-12/25 core loading.

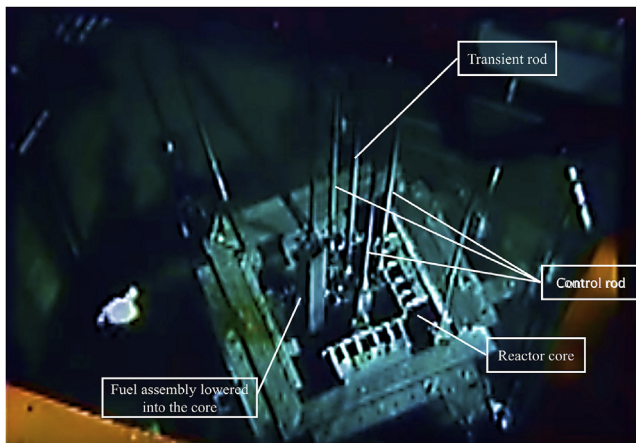


Fig. 2. SPERT-IV loading (ANL, 2011).

transient rod had an opposite operation direction. Unlike the normal fuel assembly, the control assembly contains 6 fuel plates in order to facilitate the control blades (Heffner et al., 1962; Schroeder, 1963; Crocker et al., 1963; Heuffman et al., 1963; Crocker and Stephan, 1964; Day, 2006).

The SPERT-IV experiments consisted of a series of non-destructive self-limiting tests for a variety of coolant flow conditions, initiated by step-wise insertion of positive reactivity by the quick withdrawal of the transient rod from the core central fuel assembly. A summary of all the step insertion tests appears in (Day, 2009). For most of the transients, the initial power was approximately 1 W and the thermal-hydraulic conditions corresponded to this power level. The experiments were executed in the sequence that is presented in Fig. 3. Reactivity insertion values for the tests varied in the range between 0.88 and 2.14\$, resulting in transients with initial periods of between 980 and 7 ms. The initial bulk temperature was at ambient room temperature (20 °C), the total core coolant flow rate varied between 0, 500, 1000, 2500 and 5000 gpm (corresponding to coolant velocities of 0, 0.387, 0.771, 1.929 and 3.87 m/s). The reactivity coefficients are summarized in Table 1, where due to the characteristics of the HEU fuel, the Doppler reactivity feedback is negligible. Thus, the only considerable reactivity feedback for the transient mitigation was the change in the density of the coolant. Finally, the reduced prompt neutron generation time is discussed later in subsection 3.1.

Table 1

Summary of the neutronic input parameters.

Parameter	Value
Average coolant temperature feedback at 20°C	- 0.7 ¢/°C
Average coolant temperature feedback at 35°C	- 1.2 ¢/°C
Average density/void feedback coefficient	- 41.5 ¢/%
Reduced prompt neutron generation time $\Lambda/\beta_{\text{eff}}$	$8.1 \times 10^{-3}$ s

2.2. Serpent

Serpent is a continuous energy MC neutron transport code with burnup capabilities (Leppänen, 2007). It allows modeling of complicated two- or three-dimensional geometries. This code was initially developed as an alternative to deterministic lattice codes for the generation of homogenized few-group constants for reactors analyses by nodal codes. Current analyses are performed with ENDF/B-VII.0 nuclear data evaluation. In the current study, Serpent MC is utilized as a steady state solver in order to obtain the three-dimensional power distribution in the SPERT-IV core.

2.3. THERMO-T

THERMO-T system code couples between thermal-hydraulic (TH) and neutronic point kinetics (PK) modules. The code solves the three TH conservation equations (mass, momentum, and energy) in time and space, with the capability to model any number of channels (average and hot, multichannel etc.). The neutronic module solves the power amplitude using seven equations of the PK model with one group for prompt neutrons and six groups for delayed-neutrons precursor concentrations. The radial power peaking and axial power shape are calculated using Serpent at certain given time points  $t$  during the transient (control rod extraction).

The main challenge in such self-limiting transients is the proper prediction of the evolution of the two-phase flow in the subchannel (Chatzidakis et al., 2012). The rapid and violent generation of steam in the core as a result of the reactivity insertion, as can be seen in the video taken in the facility during one of the tests (ANL, 2011), indicates the greatness of the challenge. Fig. 4 shows seven frames taken during the course of the accident progression. Fig. 4a shows the location of the different instrumentation tubes above the core and Fig. 4b represents the initial stage of the transient, where the transient rod is located at its upper most position. Fig. 4c shows the movement of the transient rod downwards and Fig. 4d shows the full extraction of the transient rod

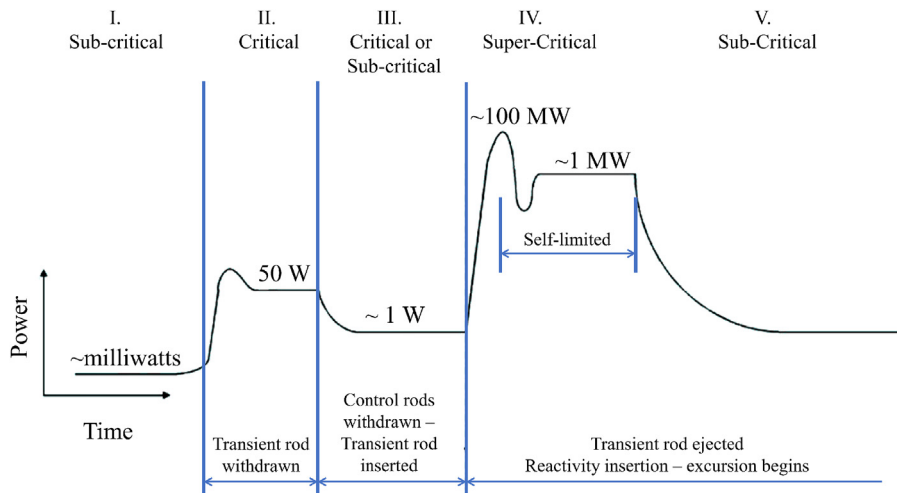


Fig. 3. SPERT-IV Reactivity insertion transient sequence (Day, 2009).

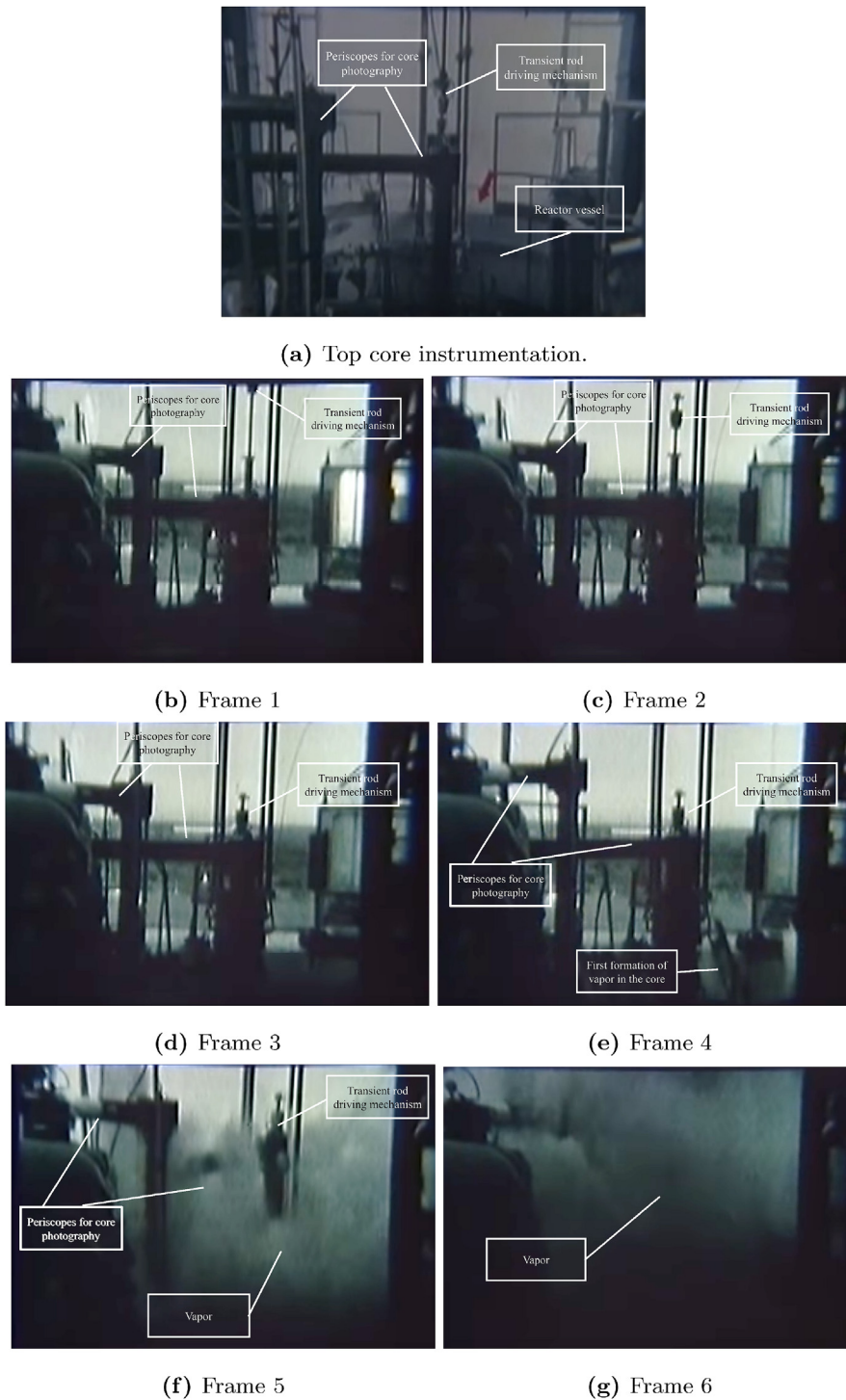


Fig. 4. Transient progression in SPERT-IV as captured by camera above the core (ANL, 2011).

(out of the core), with the driving mechanism reaching its final position. Fig. 4e shows the evolution of the vapor in the core as a result of the reactivity insertion. One can notice the vapor force that drives the periscopes upwards (Fig. 4d vs. e), with some void visible in the frame. Fig. 4f and g shows the fast eruption of vapor formed in the core.

Considering the difficulties mentioned above, previous studies 34 showed that different selection of correlation could lead to large deviation of the calculated results from the experimental data, where some combination of correlations lead to overestimation by more than 100% of the experimental data. Nevertheless, the correlation that found to be in some agreement with the experimental data still overestimated

the experimental results by about 30–50%.

In the current THERMO-T version, a set of correlations available in (Todreas and Kazimi, 1990b) is utilized for locating the point at which the local heat flux supports the bubble nucleation and the onset of significant void. The formula are presented in Eqs. (1) and (2) for Onset of Nucleate Boiling (ONB) and Onset of Significant Void (OSV), respectively,

$$\frac{1}{\Gamma} = \frac{(T_W - T_{sat})^2}{(T_W - T_{bulk})^3} \quad (1)$$

$$\Gamma = \frac{k_l h_{fg}}{8\sigma T_{sat} \nu_{fg} h_c}$$

and

$$T_{sat} - T_{bulk} = 0.0022 \left( \frac{q'' D_{Hl}}{k_l} \right), \quad Pe < 7 \times 10^4$$

$$T_{sat} - T_{bulk} = 154 \left( \frac{q''}{G \cdot C_{p_l}} \right), \quad Pe > 7 \times 10^4 \quad (2)$$

where  $T$  is the temperature of the wall ( $W$ ), coolant bulk ( $bulk$ ) and saturation ( $sat$ ),  $k_l$  is the thermal conductivity of the liquid phase,  $C_{p_l}$  is the heat capacity of the liquid phase,  $h_{fg}$  is the latent heat of vaporization,  $v_{fg}$  is the specific volume of the phase change,  $\sigma$  is the surface tension of vapor phase,  $q''$  is the heat flux of node  $i$ ,  $D_{Hl}$  is the equivalent hydraulic diameter of the channel,  $G$  is the mass flux,  $h_c$  is the heat transfer coefficient and  $Pe$  is Peclet number.

The numerical scheme implemented in THERMO-T is based on the Semi-Implicit Method for Pressure Linked Equations (SIMPLE), which provides the solution of the velocity, pressure and temperature fields along the flow channel. The solution of the three fields is then utilized

to solve the heat conduction towards the fuel center line, providing the estimation of the temperatures of the cladding surface, the interaction plenum between the clad and the fuel and finally the fuel center line. However, the formation of the steam in the channel requires the update of the different fields through the two-phase flow models. The updated scheme proposed for the treatment of the two-phase flow in THERMO-T is presented in Fig. 5.

First the SIMPLE is solved in order to obtain the velocity and pressure fields, followed by the solution of the heat balance in the  $i^{th}$  node. The solution of Eqs. (1) and (2), which is utilized to identify the evolution of the two-phase flow in the channel, is compared to the bulk temperature in the  $i^{th}$  node obtained from the heat balance solution. In case the temperature of the node exceeds the obtained solution from Eqs. (1) or (2), the code switches between the different correlation for the update of the velocity, pressure and temperature fields. In case the temperature of the node exceeds the onset of significant void (Eq. (2)), the void fraction is estimated according to Eq. (3) in the  $i^{th}$  node, and

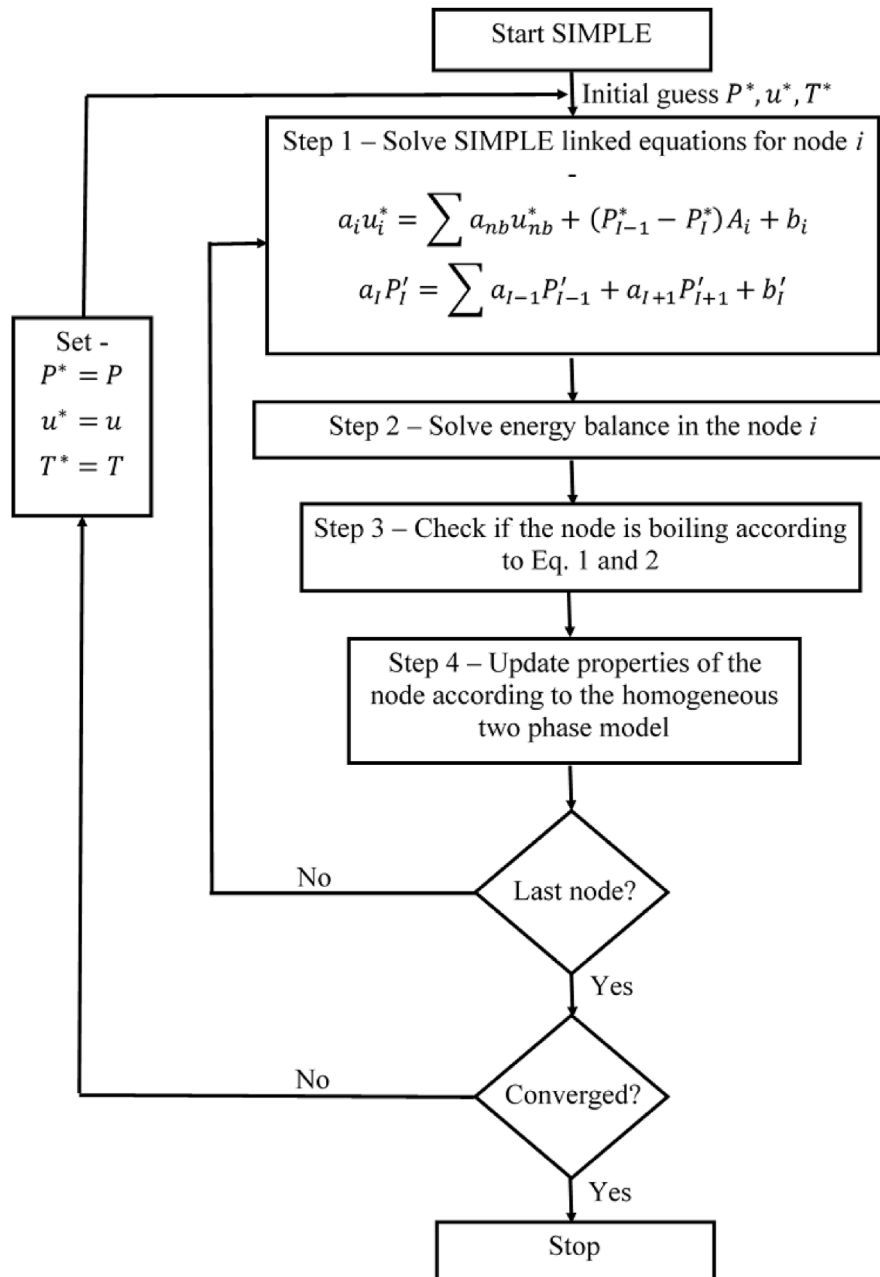


Fig. 5. THERMO-T solution scheme with two-phase flow updated capabilities.

the coolant properties are updated according to the calculated void fraction. The process is repeated until the temperature distribution of the entire channel is obtained, and continues until all the three fields are converged, followed by the advance of the time step.

$$\alpha = \frac{1}{C_0 \left( 1 + \frac{1-x\rho_v}{x\rho_l} \right) + \frac{V_{ij}\rho_v}{xG}}, \quad (3)$$

where  $x$  is the local vapor quality,  $\rho$  is the density of the liquid ( $l$ ) and vapor ( $v$ ) phases and  $V_{ij}$  is the drift-flux velocity. There are many correlations for calculation of the drift velocity and the  $C_0$  coefficients, the ones utilized in THERMO-T are the ones proposed by (Rouhani and Axelsson, 1970), i.e.,

$$C_0(x) = [1 + 0.2(1-x)] \left( \frac{9.81D_H\rho_l}{G^2} \right)^{0.25} \quad (4)$$

$$V_{ij}(x) = 1.18(1-x) \left[ \frac{9.81\sigma(\rho_l - \rho_v)}{\rho_l^2} \right]^{0.25}, \quad (5)$$

where  $x$  is the local vapor quality,  $D_H$  is the hydraulic diameter,  $G$  is the flow rate,  $\rho_l$  and  $\rho_v$  are the densities of the liquid and the vapor phases, respectively, and  $\sigma$  is the surface tension.

Finally, in light of the previous results, THERMO-T utilizes the critical heat flux correlation similar to the one available in PARET-ANL code (Chatzidakis et al., 2012). The estimation of the critical heat flux is done according to

$$q''_{CHF} = F1 \times F2 \times F3 \times F4, \quad (6)$$

where

$$F1 = 0.23 \times 10^6 + 0.094G \quad (7)$$

$$F2 = 3 + 0.01(T_{sat} - T_{bulk}) \quad (8)$$

$$F3 = 0.435 + 1.23e^{0.0093 \cdot dz/D_H} \quad (9)$$

$$F4 = 1.7 - 1.4e^{-a} \quad (10)$$

$$a = 0.532 \left( \frac{h_l - h_{bulk}}{h_v^{0.75}} \right) \left( \frac{\rho_g}{\rho_l} \right)^{-1/3}, \quad (11)$$

where  $G$  is the flow rate,  $T_{sat}$  and  $T_{bulk}$  are the saturation and coolant bulk temperatures, respectively,  $dz$  is the heated length,  $D_H$  is the hydraulic diameter,  $h_l$ ,  $h_v$  and  $h_{bulk}$  are the enthalpy of the liquid, vapor and the coolant bulk, respectively, and  $\rho_l$  and  $\rho_v$  are the densities of the liquid and vapor phases.

### 3. Results

The results section exhibit both static and transient calculations. The static comparison deals with Serpent calculation and the available static results from the SPERT-IV reactor (Woodruff et al., 1997). The transient section presents the results for a constant reactivity insertion at different coolant velocities.

#### 3.1. Static comparison

One of the features available in THERMO-T is the utilization of a realistic power distribution, calculated or measured, by an independent source, e.g., Serpent in the this work. Thus, the flux and power solver, along with its input deck and neutron data libraries first need to be validated against the static measurements available from the experiment. The Serpent results were validated versus the thermal flux distribution measured in SPERT-IV by means of cobalt wires located at positions shown in Fig. 6. In order to validate the results obtained from Serpent, the measured and calculated thermal fluxes were compared in several core positions, where the energy cutoff for thermal flux was set to 0.5 eV (Crocker and Stephan, 1964). The selected positions for

comparison were D4, D5, E4, E5, F5, and G7. This allows to test the calculation capabilities in different importance regions, where D4 and E5 are the locations of the control and transient rods (location which is most divergent from a normal cosine-shaped axial flux distribution), respectively. The comparison of the calculated and measured values are shown in Figs. 7–9. All the results are normalized to the maximal flux value in D4, E4, and F5, respectively, and to twice the maximal flux value in D5, E5 and G7, respectively, for better representation.

Generally, the results show good agreement between the calculated and the measured thermal fluxes. The largest discrepancy is observed in the reflector region, possibly due to low statistics in the simulation or the model of the grid plate at the core bottom plenum. This discrepancy in the reflector region is of little importance for the transient analysis because first, it is still absolutely small and second, the reflector contains no fissile material hence no power is generated at the bottom plate.

The second comparison between the experiment and the Serpent calculation was made on the estimation of the reduced prompt neutron generation time. The calculated values of the reduced prompt neutron generation time ( $\Lambda / \beta_{eff}$ ) are summarized in Table 2. Previous analysis of the SPERT-IV experiment, which was performed in the frame work of the IAEA working group, utilized TRIPOLI-4 for the static evaluation of the SPERT-IV experiment (IAEA, 2013). The calculated value of the reduced prompt neutron generation time estimated by TRIPOLI-4 is in good agreement with the value obtained from Serpent, as shown in Table 2. On the other hand, the two codes overestimated the value of the reduced prompt neutron generation time by about 2.5%.

#### 3.2. Reactivity insertion results

The reactivity insertion in the experimental program varied from 0.88 to 2.14\$ in step wise function. When considering the range of the reactivity insertion, it is possible to divide it into two groups, with a cut-off at 1.2\$ (IAEA, 2015). The sharp reactivity insertion (above 1.2\$) leads to dramatic increase in the amount of vapor in the core. This, in tun, leads to a very strong dependency (of the results) on the specific

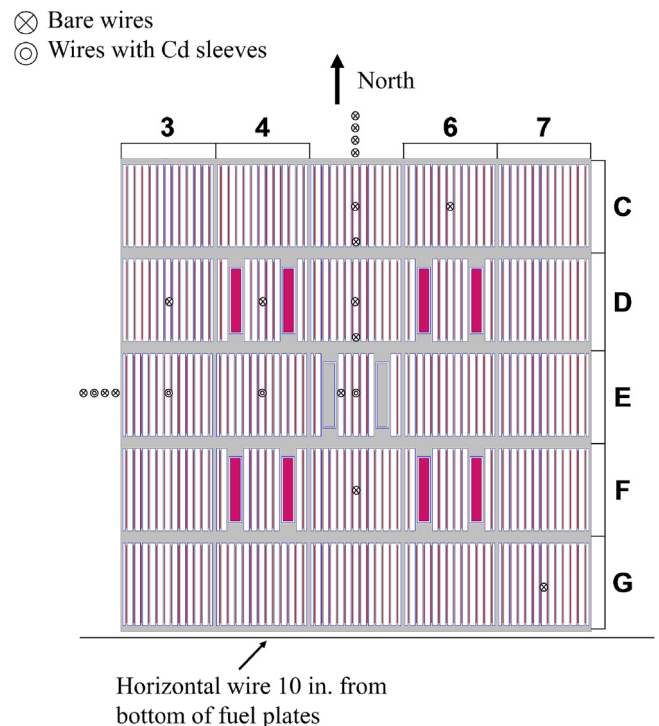


Fig. 6. Radial positions of the cobalt wires for thermal flux measures (Crocker and Stephan, 1964).

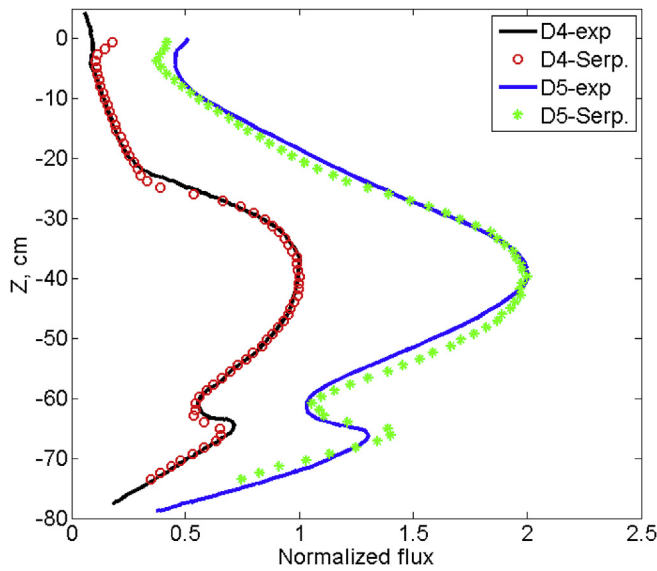


Fig. 7. Comparison of thermal flux detectors at locations D4 and D5.

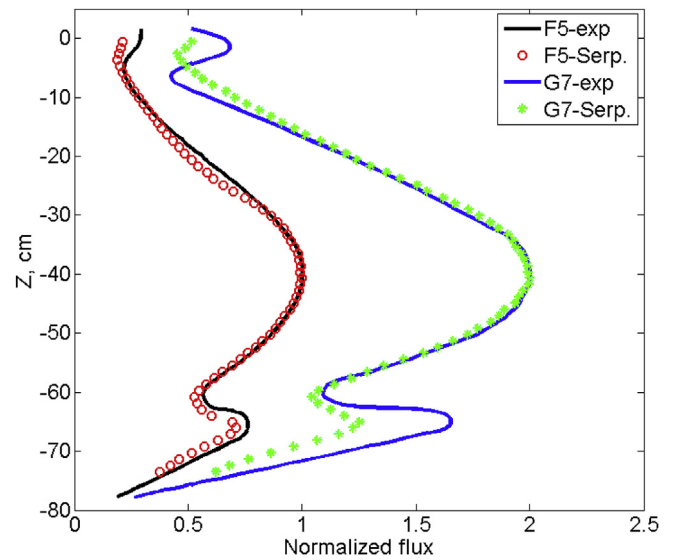


Fig. 9. Comparison of thermal flux detectors at locations F5 and G7.

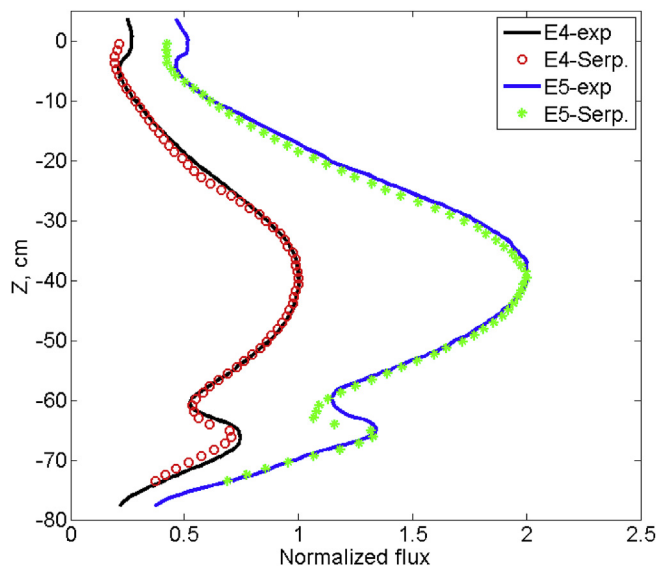


Fig. 8. Comparison of thermal flux detectors at locations E4 and E5.

correlation selected in the simulation process, mainly on the Departure from Nucleate Boiling (DNB) correlation (Chatzidakis et al., 2012). The strong dependency on the correlation was found to be most influential at high reactivity insertions (above 1.2\$). Therefore, in order to test the capabilities of the two-phase flow model, the focus in the current work is made on the low reactivity insertion, which ensure a gradual evolution of the two-phase flow. Hence, two reactivity insertions, 0.88 and 1.14\$, are considered. The initial steady-state conditions of the core prior to the transient are summarized in Table 3.

Nevertheless, when the high reactivity insertion rates are considered, previous limited analysis of the SPERT-IV experiments showed large deviations from the available experimental data. Analyses which were performed with well-established codes, such as RELAP5/MOD3 (Woodruff et al., 1997), PARET-ANL (Chatzidakis et al., 2012) and EUREKA-2/RR (Bardun et al., 2014), all presented large discrepancies in the calculated values with respect to the experimental data. Moreover, the calculated results generally follow a trend, i.e., the deviation of the calculated results (with respect to the experiment) increases as the reactivity insertion rate increases.

In addition to the different reactivity insertions, the experiments

Table 2

Comparison between calculated and measured reduced prompt neutron generation time.

	$\beta_{\text{eff}}$ [pcm]	$\Lambda$ [ $\mu$ s]	$\Lambda/\beta_{\text{eff}}$ [ms]
Serpent	$748 \pm 2$	$62.5 \pm 0.1$	$8.36 \pm 0.02$
TRIPOLI4	$768 \pm 9$	$64.0 \pm 0.2$	$8.33 \pm 0.09$
Experiment	N/A	N/A	8.1

were carried out using both forced and natural convection flow modes. The latest version of THERMO-T has yet to be equipped with a model for natural convection, thus at this stage experiments with a flow rate of 0 gmp are not examined. The results of the 0.88\$ step reactivity insertion for different mass flow rates are summarized in Figs. 10–13.

The obtained results show that THERMO-T overestimate the experimental values of the power and cladding temperature obtained from the SPERT-IV experiments. The overestimation of the results could be linked to the assumptions made in the homogeneous flow model. Additional contribution to the overestimation can result from the simplification of the neutronic model, e.g., point kinetics. THERMO-T is able to provide distribution of the void in each channel of the core. However, the point kinetics model considers only a lumped parameter (coolant density) averaged on the entire core. The average process may introduce error into the lumped parameter calculation, as the contribution or importance of void in different parts of the core may not be the same, and vary strongly between the different channels. Therefore, it is reasonable that a more detailed neutronic model coupled to an advanced thermal-hydraulic solver can potentially model the SPERT-IV experiments better. However, THERMO-T results do follow the same general trend as the experimental data, where no maximal value for both power and temperature over time is noticed.

The results of the power peak and peak cladding temperature achieved during the 1.14\$ reactivity insertion as a function of mass

Table 3

Initial steady-state conditions prior to the transient as provided to THERMO-T.

Variable	Value
Coolant inlet temperature	22.8 °C
Initial core power	1 W
Flow rate	500, 1000, 2500, 5000 [gpm]
Reactivity insertion	0.88, 1.14 \$

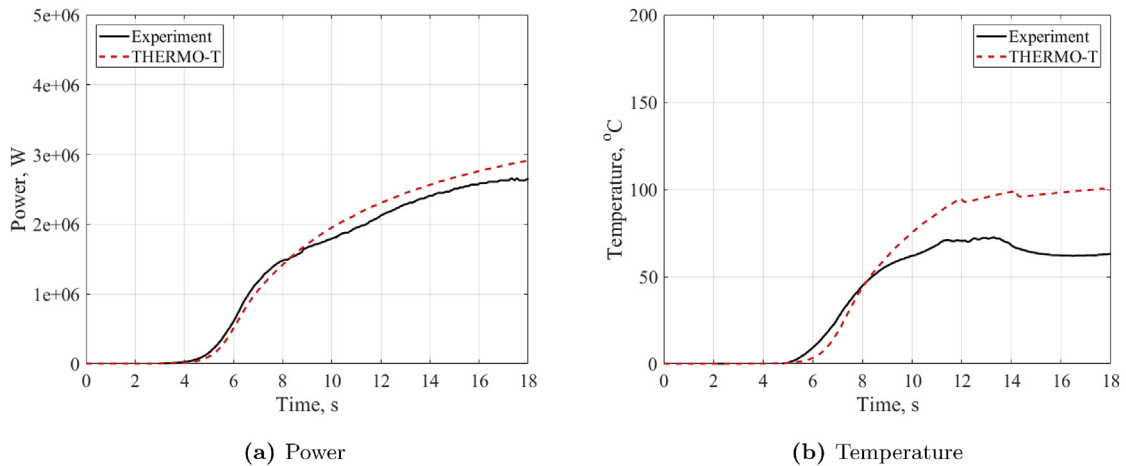


Fig. 10. Reactivity insertion of 0.88\$ for 500 gpm mass flow rate.

flow rate are summarized in Figs. 14 and 15, respectively. The calculated values of the power peak (Fig. 14) for the low mass flow rates are in well agreement with the measured data. However, as the flow rate increases, the results obtained from THERMO-T are increasingly overestimating the measurements. In the final experiment (5000 gpm), the deviation reaches about 60%. Nevertheless, the measured and calculated power peak are following the same trend, where the power peak achieved during the transient is increasing as a function of the flow rate. The peak cladding temperature obtained from the calculation (Fig. 15) overestimates the experiment values with a slight increase in deviation as the volumetric flow rate is increased. However, an additional point in Fig. 15, denoted as "unclear point", is found in table B-I in the original benchmark description (Crocker and Stephan, 1964), for the 5000 gpm flow rate, which, if considered, reduces the discrepancy between the calculated and experimental values.

Fig. 16 shows an example of the power and clad temperature progression over time during the 1.14\$ reactivity insertion at a flow rate of 1000 gpm. The cladding temperature prediction results of THERMO-T overestimate the experimental values by a factor of two, where the average error of the power estimation was about 30% when the core reached a new steady state. However, the general trend of the calculated values is similar to the experimental data, a rise to a peak value and then stabilization to a new steady state.

These results and the results from previous studies (Woodruff et al., 1997; Chatzidakis et al., 2012; Bardun et al., 2014) provide an indication that the two-phase flow models are not providing a good

estimation on the generation of steam in the channel. Unfortunately, the benchmark does not provide a continuous time scale of the transient (i.e., the time stamps given in the benchmark do not correspond to the time passed since initiation of the transient), making it impossible to compare the points where the power and temperature start to rise, and examine the generation of steam in the channels. A comparison of the curves shapes (Figs. 10–13 and 16) shows that the evolution of the calculated void in the channel is not as rapid as in the experiment, leading to a slower feedback, which leads to a higher value. Furthermore, the point kinetics model may not be accurate for this type of problem, since the assumption of average values for the calculation of the coolant density reactivity feedback might introduce an additional error into the model.

Finally, it seems that the overestimation of the power and cladding temperature peaks is probably due to three-dimensional coupled neutronics and thermal-hydraulic effects, which need to be further investigated. Furthermore, additional investigation of the boiling prediction model is needed as well as the utilization of appropriate correlations for highly voided core conditions.

#### 4. Conclusion

This paper presents the latest developments in the continuous effort to develop a three-dimensional coupled neutronic and thermal-hydraulic system code package for RR analysis, which is based on the Serpent MC code, for few group constant generation, a three-

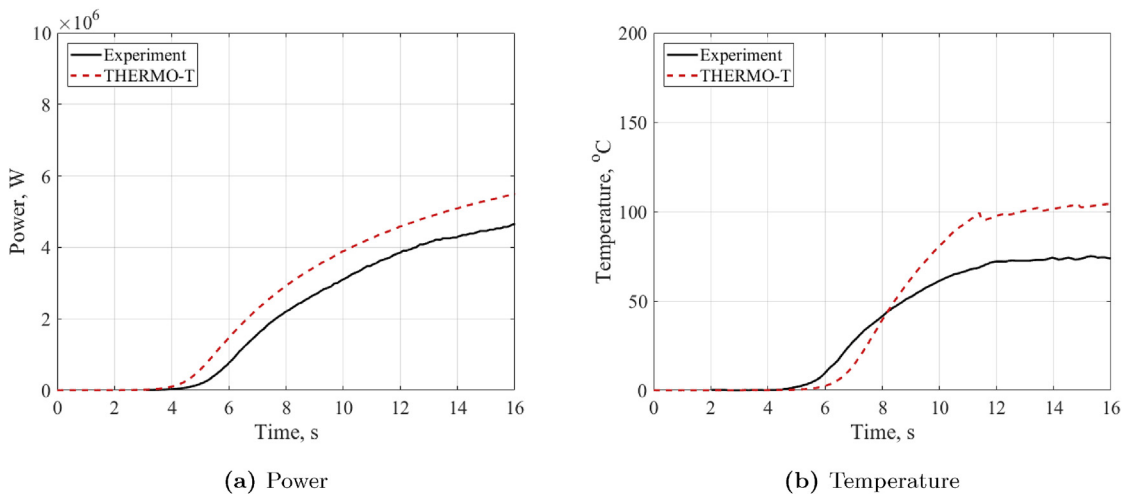
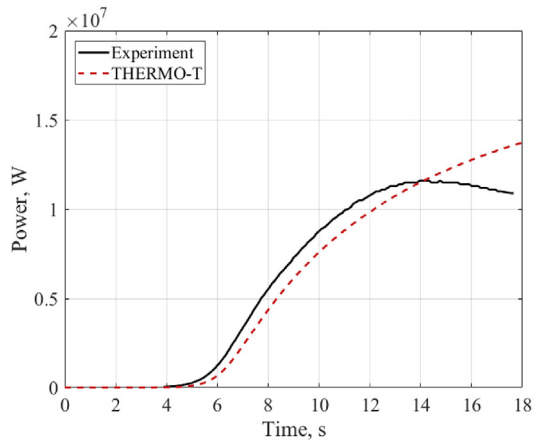
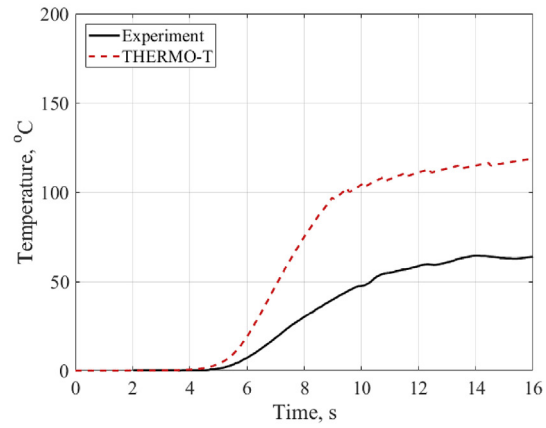


Fig. 11. Reactivity insertion of 0.88\$ for 1000 gpm mass flow rate.

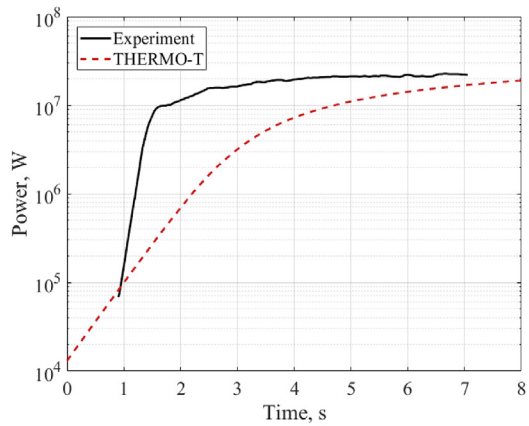


(a) Power

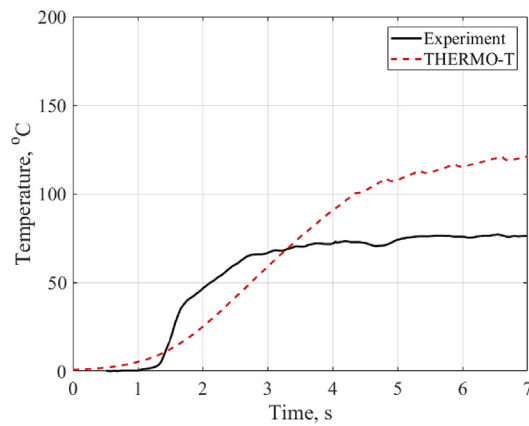


(b) Temperature

Fig. 12. Reactivity insertion of 0.88\$ for 2500 gpm mass flow rate.



(a) Power



(b) Temperature

Fig. 13. Reactivity insertion of 0.88\$ for 5000 gpm mass flow rate.

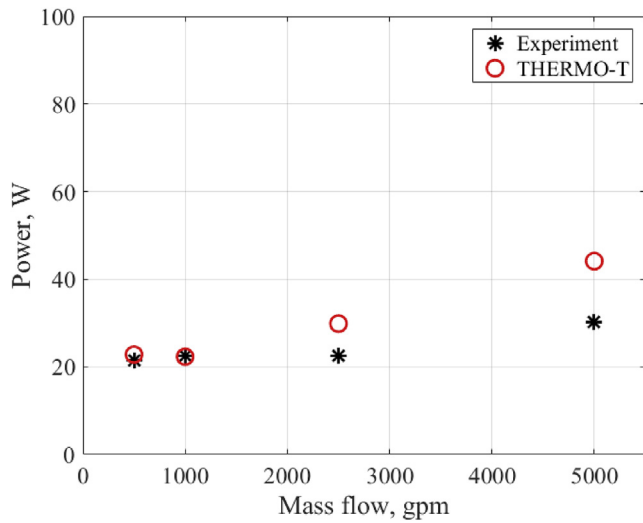


Fig. 14. Peak power measured for 1.14\$ reactivity insertion for various mass flow rates.

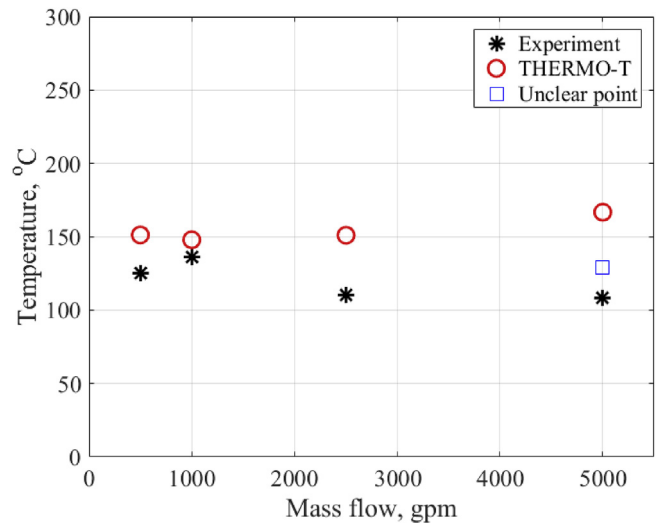


Fig. 15. Peak cladding temperature measured for 1.14\$ reactivity insertion for various mass flow rates.

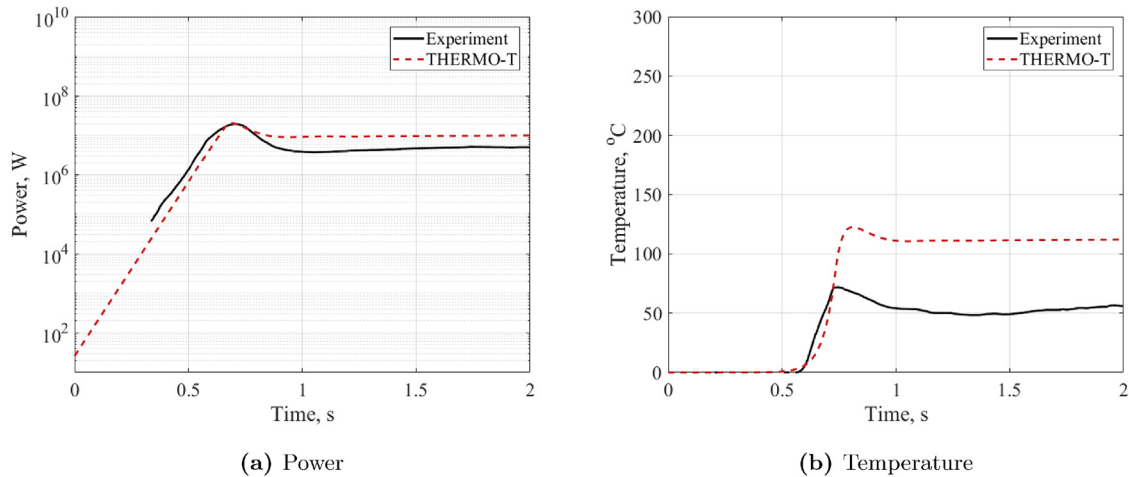


Fig. 16. Reactivity insertion of 1.14\$ for 1000 gpm mass flow rate.

dimensional neutron diffusion solver of the DYN3D code, and THERMO-T for the estimation of the thermal-hydraulic properties of the reactor. The first stage was completed recently, with the static and dynamic benchmark verification of the proposed system code versus the 10 MW<sub>th</sub> IAEA MTR benchmark. However, this benchmark tends to be considered obsolete to some extent for code validation, especially in light of the recent publication of the IAEA experimental benchmark data bank. From the available experimental reactors data, the system that was selected for validation purposes was the experimental program carried out in the SPERT-IV facility.

Modeling of the SPERT-IV experiments required modifications to the THERMO-T calculation scheme. This work focuses on the introduction of the basic two-phase flow models into the THERMO-T system code. At this stage, the homogeneous two-phase flow model, with a commonly utilized correlation for the estimation of the onset of nucleate boiling, the onset of the significant void point, the void fraction correlation, and the drift-flux velocity model for the updated velocity field were implemented. The selection of the models follows the traditional models used in other transient channel codes. This is done in order to test these models against an experimental benchmark, which was designed in such way that only the void reactivity coefficient is mitigating the transient.

Originally, the SPERT-IV benchmark problem was divided into two parts. The first part deals with the static thermal flux distribution comparison in different locations inside the core, along with the reduced prompt neutron generation time, which is a key parameter for the transient analysis. The results, which are presented in subsection 3.1, show excellent agreement between results obtained from Serpent and the measured values from the benchmark specification (Figs. 7–9). Small discrepancies are observed in the reflector regions, which could result from low statistics in the Serpent simulations or modeling accuracy of the egg-crate grid at the core bottom, as the bottom reflector is modeled as homogeneous media. The second part of the static benchmark compared the reduced prompt neutron generation time between Serpent, TRIPOLI-4 and the benchmark value (Table 2). It is found that while Serpent and TRIPOLI-4 predict almost the same value, both codes slightly overestimate the value given in the benchmark. This could potentially lead to discrepancies in the transient modeling.

The second part of the benchmark treats the dynamic response analysis of the reactor to a step-wise reactivity insertion. For this stage, three-dimensional power shapes, obtained from Serpent, are utilized in THERMO-T in a classical two-channel model (hot and average) with different mass flow rates for different rates of reactivity insertion. The benchmark contains information regarding reactivity insertion of different magnitude, varying from 0.88\$ to more than 2\$. The benchmark results are divided into two subgroups, i.e., low and high reactivity

insertion (cut-off at 1.2\$). In the present analysis, two types of low reactivity insertion are considered (0.88\$ and 1.14\$), as the high reactivity insertion results in rapid evaporation of the coolant, which demands a special treatment which is not yet implemented in THERMO-T.

The results obtained for this first simulation of the SPERT-IV experiments show a large deviation between the experimental and calculated results for all the cases. The differences are visible through the entire transient period, with large temperature deviation (for 0.88\$ - Figs. 10–13 and for 1.14\$ Figs. 15 and 16). However, the trend of the calculated results is similar to the trend observed in the experimental system. The results presented in this paper fall in line with results obtained from previous evaluation made with PARET-ANL and RELAP5 of the SPERT-IV experiments, where large discrepancies were also observed. The unique combination of HEU fuel and large reactivity insertions makes the SPERT-IV a good evaluation problem for the thermal-hydraulic and neutronic models.

Considering the presented results, it is reasonable to assume that the first (most basic) approach for two-phase modeling (homogeneous model) is probably not sufficient for the modeling of the SPERT-IV experiments, and a more sophisticated model is required. Therefore, at this stage, the utilization of the separate flow model is considered in the future version of THERMO-T. Furthermore, the estimation of the onset of significant void requires revisiting, as the currently available correlation may not be sufficient. However, the large discrepancies between the calculated and measured results may be attributed to the neutronic model. The utilization of the point kinetics model may not be suitable in such an unevenly distributed void system (higher in the middle, lower at the periphery), and a more elaborated model is needed, such as three-dimensional diffusion model, which is the goal for the current activity.

## References

- D'Auria, F., Bousbia-Salah, A., 2006. Accident analysis in research reactors. In: 15th Pacific basin Nuclear Conference, Sydney, Australia, Oct. 15-20 2006, pp. 88–93.
- Adorni, M., Bousbia-salah, A., D'Auria, F., Hamidouche, T., 2006. Application of Best Estimate thermalhydraulic codes for the safety analysis of research reactors. In: International Conference on Nuclear Energy for New Europe 2006, Portoroz, Slovenia, Sep. 18-21 2006.
- Adorni, M., Bousbia-salah, A., D'Auria, F., Hamidouche, T., 2007. Accident analysis in research reactors. In: International Conference on Nuclear Energy for New Europe 2007, Portoroz, Slovenia, Sep. 10-13 2007.
- ANL, 2011. SPERT - destructive test. <http://www.youtube.com/watch?v=0FIhafVX.6I>
- Bardun, N.H., Altaf, M.H., Motalab, M.A., Mahmood, M.S., Khan, M.J.H., 2014. Modeling SPERT-IV reactivity initiated transient test in EUREKA-2/RR code. International Journal of Nuclear Energy 2014, 1–8. <https://doi.org/10.1155/2014/167426>.
- Chatzidakis, S., Ikonopoulou, A., Day, S., 2012. PARET-ANL modeling of a SPERT-IV experiment under different departure from nucleate boiling correlation. Nucl.

- Technol. 177 (0), 119–131.
- Chatzidakis, S., Ikononopoulos, A., Ridikas, D., 2013. Evaluation of RELAP5/MOD3 behavior against loss of flow experimental results from two research reactor facilities. *Nucl. Eng. Des.* 255, 321–329.
- Chatzidakis, S., Hainoun, A., Doval, A., Alhabet, F., Francioni, F., Ikononopoulos, A., Ridikas, D., 2014. A comparative assessment of independent thermal-hydraulic models for research reactors: the RSG-GAS case. *Nucl. Eng. Des.* 268 (0), 77–86. <http://www.sciencedirect.com/science/article/pii/S0029549313007000> <https://doi.org/10.1016/j.nucengdes.2013.11.076>.
- Costa, A.L., Pereira, C., Silva, C.A.M., Reis, P.A.L., Fortini, M.A., Soares, H.V., Mesquita, A., 2011. Safety studies and general simulations of research reactors using nuclear codes. In: Tsvetkov, P. (Ed.), *Nuclear Power*; Chap. 2. InTech, Rijeka, pp. 21–42. <https://doi.org/10.5772/17411>.
- Crocker, J.G., Stephan, L.A., 1964. Reactor Power Excursion Test in the SPERT IV Facility. Tech. Rep. U.S. AEC Technical Report Ido-17000. Phillips Petroleum Company.
- Crocker, J.G., Koch, J.E., Martinson, Z.R., McGlinsky, A.M., Stephan, L.A., 1963. Nuclear Start-up of the SPERT IV Reactor. Tech. Rep. U.S. AEC Technical Report Ido-16905. Phillips Petroleum Company.
- Day, S., 2006. The Use of Experimental Data in an MTR Type Nuclear Reactor Safety Analysis. Ph.D. thesis. McMaster University.
- Day, S., 2009. SPERT-iv Benchmark Specification, IAEA Coordinated Research Project 1496: Innovative Methods in Research Reactor Analysis. Tech. Rep. IAEA-crp-1496. IAEA.
- Fratoni, M., 2017. Criticality benchmark of the molten salt reactor experiment. In: *Molten Salt Reactor Workshop 2017*.
- Hainoun, A., Doval, A., Umbehaun, P., Chatzidakis, S., Ghazi, N., Park, S., Mladin, M., Shokr, A., 2014. International benchmark study of advanced thermal hydraulic safety analysis codes against measurements on IEA-R1 research reactor. *Nucl. Eng. Des.* 280 (0), 233–250. <http://www.sciencedirect.com/science/article/pii/S0029549314004269> <https://doi.org/10.1016/j.nucengdes.2014.06.041>.
- Hamidouche, T., Bousbia-Salah, A., Adorni, M., D'Auria, F., 2004. Dynamic calculations of the IAEA safety MTR research reactor benchmark problem using RELAP5/3.2 code. *Ann. Nucl. Energy* 31 (12), 1385–1402. <http://www.sciencedirect.com/science/article/pii/S0306454904000581> <https://doi.org/10.1016/j.anucene.2004.03.008>.
- Hamidouche, T., Bousbia-Salah, A., Si-Ahmed, E.K., D'Auria, F., 2008. Overview of accident analysis in nuclear research reactors. *Prog. Nucl. Energy* 50 (1), 7–14. <http://www.sciencedirect.com/science/article/pii/S0149197007002326> <https://doi.org/10.1016/j.pnucene.2007.11.089>.
- Heffner, R.E., Morris, E.L., Jones, D.T., Seaman, D.R., Shane, M.K., 1962. SPERT-iv Facility. Tech. Rep. U.S. AEC Technical Report Ido-16745. Phillips Petroleum Company.
- Heuffman, J.R., Nyer, J.R., Schroeder, F., 1963. Quarterly Technical Report, SPERT Project: January, February, March, 1963. Tech. Rep. U.S. AEC Technical Report Ido-16893. Phillips Petroleum Company.
- Horelik, N., Herman, B., Forget, B., Smith, K., 2013. Benchmark evaluation and validation of reactor simulation (BEAVRS). In: *Proc. Int. Conf. Mathematics Ad Computational Methods Applied to Nuclear Science*.
- IAEA, 1980. Research Reactor Core Conversion from the Use of High-enriched Uranium to the Use of Low Enriched Uranium Fuels Guidebook. Tech. Rep. IAEA-tecdoc-233. International Atomic Energy Agency.
- IAEA, 1992. Research Reactor Core Conversion Guidebook. Tech. Rep. IAEA-tecdoc-643-v1. International Atomic Energy Agency.
- IAEA, 2007. Use and Development of Coupled Computer Codes for the Analysis of Accidents at Nuclear Power Plants. Tech. Rep. IAEA-tecdoc-1539. International Atomic Energy Agency.
- IAEA, 2008. Safety Analysis for Research Reactors. Tech. Rep. Safety Report Series 55. International Atomic Energy Agency.
- IAEA, 2013. IAEA CRP 1496 (2008-2013) Innovative Methods in Research Reactors Analysis: Benchmark against Experimental Data on Neutronics and Thermalhydraulics Computational Methods and Tools for Operation and Safety Analysis of Research Reactors. Tech. Rep. IAEA-crp-1496. International Atomic Energy Agency.
- IAEA, 2015. Research Reactor Benchmarking Database: Facility Specification and Experimental Data. Tech. Rep. Technical Reports Seris No. 480. International Atomic Energy Agency.
- Leppänen, J., 2007. Development of a New Monte Carlo Reactor Physics Code. Ph.D. thesis. Helsinki University of Technology.
- Margulis, M., Gilad, E., 2015. Analysis of protected RIA and LOFA in plate type research reactor using coupled neutronics thermal-hydraulics system code. In: *The 16th International Topical Meeting on Nuclear Reactor Thermal Hydraulics (NURETH-16)*, Chicago, Illinois, August 30-September 4.
- Margulis, M., Gilad, E., 2016a. Monte Carlo and nodal neutron physics calculations of the IAEA MTR benchmark using Serpent/DYN3D code system. *Prog. Nucl. Energy* 88, 118–133.
- Margulis, M., Gilad, E., 2016b. Development and verification of a dynamic system code THERMO-T for research reactor accident analysis. *Nucl. Technol.* 196, 377–395.
- Margulis, M., Blaise, P., Gabrielli, F., Gruel, A., Mellier, F., Gilad, E., 2017. The path for innovative severe accident neutronics studies in ZPRs. Part I.1 - analysis of SNEAK-12A experiments for core disruption in LMFBRs. *Prog. Nucl. Energy* 94, 106–125.
- Margulis, M., Blaise, P., Gilad, E., 2018. Modeling representative Gen-IV molten fuel reactivity effects in the ZEPHYR fast/thermal coupled ZPRs. Part 1 - assembly level. *Int. J. Energy Res.* 42 (5), 1950–1972. <https://doi.org/10.1002/er.3991>. <https://onlinelibrary.wiley.com/doi/abs/10.1002/er.3991>. <https://onlinelibrary.wiley.com/doi/pdf/10.1002/er.3991>.
- NEA, 2017. International Handbook of Evaluated Reactor Physics Benchmark Experiments. Tech. Rep. NEA/NSC/DOC(2006)1, NEA No. 7329. NEA.
- Rouhani, S.Z., Axelsson, E., 1970. Calculation of void volume fraction in the subcooled and quality boiling regions. *Int. J. Heat Mass Tran.* 13 (0), 383–393.
- Schroeder, F., 1963. Quarterly Technical Report, SPERT Project: July, August, September, 1962. Tech. Rep. U.S. AEC Technical Report Ido-16829. Phillips Petroleum Company.
- Todreas, N.E., Kazimi, M.S., 1990a. Nuclear Systems II: Elements of Thermal Hydraulic Design. Hemisphere Publishing Corporation.
- Todreas, N., Kazimi, M., 1990b. Nuclear Systems I: Thermal Hydraulic Fundamentals. Taylor & Francis ISBN 9780415802871.
- Woodruff, W.L., Hanan, N.A., Mates, J.E., 1997. A comparison of the RELAP5/MOD3 and PARET/ANL codes with the experimental transient data from the SPERT-IV D-12/25 series. In: *Abstracts and Papers of the 1997 International RERTR Meeting*. Argonne National Laboratory.